Published in final edited form as:
Cancer Immunol Res. 2014 January 1; 2(1): 27–36. doi:10.1158/2326-6066.CIR-13-0087.

Regression of metastatic Merkel cell carcinoma following transfer of polyomavirus-specific T cells and therapies capable of re-inducing HLA class-I

Aude G. Chapuis[1,*], **Olga K. Afanasiev**[2,3,*], **Jayasri G. Iyer**[3], **Kelly G. Paulson**[2,3], **Upendra Parvathaneni**[6], **Joo Ha Hwang**[7], **Ivy Lai**[1,8], **Ilana M. Roberts**[1,9], **Heather L. Sloan**[1], **Shailender Bhatia**[10], **Kendall C. Shibuya**[1], **Ted Gooley**[1], **Cindy Desmarais**[11], **David M. Koelle**[3,4,5,12,13], **Cassian Yee**[1,8,**], and **Paul Nghiem**[2,3,**]

[1]Program in Immunology, Fred Hutchinson Cancer Research Center (FHCRC), Seattle, WA, USA

[2]Department of Pathology, University of Washington, Seattle, WA, USA

[3]Department of Medicine (Dermatology), University of Washington, Seattle, WA, USA

[4]Department of Laboratory Medicine, University of Washington, Seattle, WA, USA

[5]Department of Global Health, University of Washington, Seattle, WA, USA

[6]Division of Radiation Oncology, UWMC, Seattle, WA, USA

[7]Division of Gastroenterology, UWMC, Seattle, WA, USA

[10]Department of Medicine (Medical Oncology), University of Washington, Seattle, WA, USA

[11]Adaptive Biotechnologies, Seattle, WA, USA

[12]Vaccine and Infectious Disease Division, FHCRC, Seattle, WA, USA

[13]Benaroya Research Institute, Seattle, WA, USA

Abstract

Merkel cell carcinoma (MCC) is an aggressive skin cancer that typically requires the persistent expression of Merkel cell polyomavirus (MCPyV) oncoproteins that can serve as ideal immunotherapeutic targets. Several immune evasion mechanisms are active in MCC including down-regulation of HLA class-I expression on tumor cells and dysfunctional endogenous MCPyV-specific CD8 T cell responses. To overcome these obstacles, we combined local and systemic immune therapies in a 67-year-old man, who developed metastatic MCPyV-expressing MCC. Intralesional IFNβ-1b or targeted single-dose radiation was administered as a pre-conditioning strategy to reverse the down-regulation of HLA-I expression noted in his tumors and to facilitate the subsequent recognition of tumor cells by T cells. This was followed by the adoptive transfer of *ex vivo* expanded polyclonal, polyomavirus-specific T cells as a source of reactive antitumor immunity. The combined regimen was well-tolerated and led to persistent up-regulation of HLA-I expression in the tumor and a durable complete response in two of three

[**]To whom correspondence should be addressed: Paul Nghiem, MD, PhD, Professor, Division of Dermatology UWMC, 850 Republican Street, Box 358050, Seattle, WA 98195, Tel: +1 206 221 2632, Fax: +1 206 221 4394, pnghiem@uw.edu. Cassian Yee, MD, Professor, Dept. of Melanoma Medical Oncology, Dept. of Immunology Unit 0430, MD Anderson Cancer Center, 1515 Holcombe Blvd. Unit: 904, Houston, TX 77030, Tel: +1 713 563 5272, Fax: +1 713 563 3424, cyee@mdanderson.org.
[8]Current address: Melanoma Medical Oncology, MD Anderson Cancer Center, Houston, TX, USA.
[9]Current address: Surgery Branch, NIH, Bethesda, MD, USA.
[*]Contributed equally.

Conflict of Interest:
C.D. is employed by Adaptive Biotechnologies. The rest of the authors have no conflicts to disclose.

metastatic lesions. Relative to historical controls, the patient experienced a prolonged period without development of additional distant metastases (535 days compared to historic median of 200 days, 95% confidence interval = 154–260 days). The transferred $CD8^+$ T cells preferentially accumulated in the tumor tissue, remained detectable and functional for >200 days, persisted with an effector phenotype, and exhibited evidence of recent *in vivo* activation and proliferation. The combination of local and systemic immune stimulatory therapies was well-tolerated and may be a promising approach to overcome immune evasion in virus-driven cancers.

Introduction

Merkel cell carcinoma (MCC) represents a highly aggressive neuroendocrine skin malignancy with a high disease-associated mortality, early metastatic disease, and a high propensity for recurrence after initial treatment. The cause-specific mortality ranges from 23–80% at five years, thus making it three times as lethal as melanoma (1). The Merkel cell polyomavirus (MCPyV) is clonally integrated into at least 80% of MCC tumors and produces the viral T-antigen (T-Ag) oncoproteins that are persistently expressed by MCC and are necessary for the survival and proliferation of tumor cells (2–5). Compared to mammalian tumor-associated antigens (TAAs) that all have some degree of expression within normal tissue, MCPyV T-Ag expression is restricted to MCC, is a foreign antigen not subject to T cell self-tolerance mechanisms, and is thus an optimal target for immunotherapy. Since no viral particles are formed in the tumor cells, antiviral agents are inefficient (6).

As adoptive transfer has demonstrated clinical benefit for both viral and endogenous tumor antigens (7–9), we sought to apply the use of antigen-specific T cells to target the MCPyV large T-Ag (LT-Ag) oncoprotein. The HLA-A*2402-restricted MCPyV $LT\text{-}Ag_{92\text{-}101}$-specific T cells (hereafter referred to as MCPyV-specific cells) were identified in a patient with metastatic MCC (10). These MCPyV-specific T cells, when isolated from tumors or PBMC of MCC patients, are largely dysfunctional and exhibit an immune inhibitory ($PD\text{-}1^+$/$Tim3^+$) phenotypic profile (11). We hypothesized that *ex vivo* generation of polyclonal MCPyV-specific T cells may augment the probability of including and expanding cells that had an increased potential for proliferation, function and persistence after transfer as evidenced in murine and nonhuman primate models (12, 13).

Similar to the observations in other virus-associated cancers, HLA class-I (HLA-I) downregulation is an immune escape mechanism present in the majority of MCC tumors (14–16). Single-dose low-dose radiation has been shown to up-regulate cell surface HLA-I expression (17). Data from murine models suggest that single-dose radiation is more effective than fractionated radiation in promoting tumor immunity, since the latter may suppress the function of lymphocytes that are recruited to the tumor (18). Furthermore, interferons (IFN) direct the up-regulation of HLA-I (19), and intralesional administration of IFNβ has been observed to promote immune responses in MCC (14, 20).

Here we investigated whether adoptive transfer of polyclonal MCPyV-specific $CD8^+$ T-cells following HLA-I upregulation strategies (intralesional IFNβ or local, single-fraction radiotherapy) could safely establish persistent anti-MCC responses, migrate to tumor tissue and induce regression of MCPyV-positive, HLA-I-deficient MCC metastases.

Case Report

A 67-year-old man with chronic renal failure secondary to a nephrectomy for renal cell carcinoma (RCC) at the age of 50 presented with a 1.6 cm (in largest dimension) MCC lesion on his left upper thigh and a negative sentinel node biopsy (AJCC stage IA). He

underwent a wide local excision followed by 50 Gy of fractionated local radiation to the primary site. Eight months later while still asymptomatic, a surveillance whole body positron emission tomography (PET) scan detected a 2.9 × 1.8cm lesion adjacent to the pancreatic head. Merkel polyomavirus-specific CD8 T cells were identified in the patient's tumor-infiltrating lymphocytes (TIL) and peripheral blood using a MCPyV-tetramer (10) (Suppl. Fig. S1). The patient underwent leukapheresis to allow MCPyV-specific T cells to be harvested. The patient was enrolled in a single-patient clinical trial of autologous T-cell therapy for MCC (FHCRC protocol #2558). Both the primary tumor and pre-treatment metastasis were confirmed to be classical MCC by dot-like cytokeratin-20 staining. Both lesions expressed the MCPyV T-Ag, while HLA-I expression was absent or sparse. Two additional metastases in the pancreatic head and neck appeared in the 137 days prior to the initiation of therapy.

The patient underwent three rounds of treatment (Fig. 1). Intralesional IFNβ-Ib (3×10^6 IU) was first administered per endoscope to the largest of the three detectable pancreatic metastases (designated as metastasis A). After 24 hours, the patient received an infusion of $10^{10}/m^2$ MCPyV tetramer-specific polyclonal $CD8^+$ T cells followed by low-dose subcutaneous (s.c.) IL-2 (2.5×10^5 IU/m^2) twice daily for 14 days as a means to increase T-cell persistence (21). Thirty-seven days later, a single 8 Gy fraction of radiation was delivered to all three remaining lesions (designated as metastases A, B, and C) followed by a second infusion of $10^{10}/m^2$ MCPyV-specific $CD8^+$ T cells and low-dose s.c. IL-2. On day 148 after the first infusion, metastasis B was injected with IFNβ-1b followed by a third cell infusion and low-dose s.c. IL-2 × 14 days. The patient experienced low-grade fevers and a transient, <72 hours grade 1–2 lymphopenia after each infusion, consistent with the expected immediate toxicities associated with T cell infusions (22, 23). No changes in end organ function, inflammation- or autoimmune-related complications were observed. As detailed in the Results section, follow up scans showed no evidence of new distant disease until 535 days after the original pancreatic metastasis was detected. At that time the patient developed new brain lesions that he declined to work-up or treat. The patient died one month later without additional therapeutic interventions.

Methods

Clinical protocol and patient characteristics

All clinical investigations were conducted according to the Declaration of Helsinki principles. The single-patient protocol #2558 (described above) was approved by the FHCRC Institutional Review Board and the U.S. Food and Drug Administration. The patient provided written informed consent.

Isolation and expansion of MCC-specific CTLs

Peripheral blood mononuclear cells (PBMC) were collected by leukapheresis and all ensuing *ex vivo* manipulations involving processing of products destined for infusion were performed in the cGMP Cell Processing Facility (CPF) of the FHCRC based on a protocol established for *in vitro* enrichment of low frequency antigen-specific cytotoxic T lymphocytes (CTL; ref. 24, 25). To facilitate the isolation of antigen-specific CTL, PBMC were depleted of $CD25^+$ T-cells to eliminate regulatory T-cells (26) (Miltenyi Biotec Inc.), and stimulated twice for 7–10 days with HLA-A*2402-restricted MCPyV LT-$Ag_{92\text{-}101}$ peptide (CPC Scientific)-pulsed autologous dendritic cells (DC). Each stimulation was supplemented with the γ_c-chain cytokines IL-2 (10 IU/ml), IL-7 (5 ng/ml) and IL-21 (30 ng/ml). Cultures that contained >5% specific $CD8^+$ T-cells assessed by tetramer stains were clinically-grade sorted (BD Influx cell sorter, BD Biosciences) before expansion to sufficient numbers for infusion as previously described (21,27,28). Cell products bound the

MCPyV LT-$Ag_{92\text{-}101}$ peptide-HLA tetramer, secreted IFNγ and lysed MCPyV LT-$Ag_{92\text{-}101}$-pulsed FUJI ($A24^+$ cell line) pulsed with 10μg/ml peptide (Suppl. Fig. 2).

T-cell tracking by HLA-peptide tetramers

Tetramers (produced by the FHCRC immune monitoring core facility) were used to detect transferred MCPyV LT-$Ag_{92\text{-}101}$-specific $CD8^+$ T-cells in PBMCs collected after infusions. The sensitivity of the tetramer is 0.05% of total $CD8^+$ T-cells. Persistence after infusions was calculated as the last time-point at which $tetramer^+$ T-cells were detected at 2x background levels or ≥0.05%.

Flow Cytometry

Blood samples were collected at the indicated timepoints, and the PBMC were isolated by Ficoll-Hypaque gradient and cryopreserved. Cells that bound tetramer were analyzed by flow cytometry after staining with fluorochrome-conjugated mAbs to CD14, CD16, CD19 (dump channel), CD8, CD4, CD137, CD28, CD127, CD62L, CCR7, PD-1 and TIM-3 (BD-Pharmingen). Intracellular cytokine production of IFNγ, TNFα and IL-2 by cells responding to *in vitro* stimulation with MCPyV LT-$Ag_{92\text{-}101}$ peptide for 4–5 hours were performed as described (29). Intranuclear expression of Ki-67 was assessed after permeabilization (eBioscience). Cells were analyzed on an LSRII cytometer (Becton Dickinson) using FACS-Diva software. Multiparametric flow cytometry staining, acquisition and analyses were performed on all samples in a batch on the same day and one negative control for each parameter was used. As the percentages of $tetramer^+$ T cells in the samples are often low, this method dedicated the majority of the PBMC for sample analyses.

Tracking polyclonal T-cells using high-throughput TCRβ chain DNA sequencing

A pool of primers to all V and J pairs specifically designed to amplify the complete VDJ junction region, were designed such that only the minimal region (60 nucleotides) containing the antigen-specific nucleotide information for each TCRβ CDR3 could be amplified and sequenced using the immunoSEQ assay (Adaptive Biotechnologies) (30). Using genomic DNA isolated from the blood and tumor samples as template, this method was used to capture the frequency of individual TCRs in biologic samples with accurate reproducibility and a sensitivity of 1/100,000 TCR-containing lymphocytes (31, 32). DNA from the blood and tumor samples was prepared using the DNeasy Blood & Tissue Kit (Qiagen). Source of available cells for DNA extraction included: the tetramer-sorted infusion product, cryopreserved PBMC derived using Ficoll isolation, phytohemagglutinin and IL-2 expanded TIL isolated from the primary tumor, and freshly isolated cells from the pancreatic metastatic tumor biopsy following immune therapy treatment. Results of individual TCR clonotypes are expressed as a percent of all productive, in-frame TCRs sequenced.

Immunohistochemistry

Anti-CD8 clone 4B11 (Novocastra, Newcastle, UK), anti-MCPyV T-Ag (5), and anti-HLA-I clone EMR8-5 (MBL International, Woburn, MA) were used at 1:200, 1:4000 and 1:200 dilutions, respectively, after heat-induced epitope retrieval. Specimens were assessed for MCPyV T-Ag and HLA-I expression and scored using the Allred method (33). An Allred score of 0–1.5 was considered negative (0), 2–5.5 weak (+), 6–7.5 moderate (++), and 8 strong (+++). Peritumoral and intratumoral CD8 infiltrates were scored separately as previously described (14). The numbers of $CD8^+$ cells were assessed and expressed on a 0 to 5 scale with a mean of 0, 90, 306, 508, 675, 732+ CD8s/ mm^2, respectively. Intratumoral CD8 lymphocytes were surrounded by tumor cells only with no visualized contact with stroma.

Statistical Analysis

The observed time between the first metastasis and the second metastasis for 49 patients was available and these data were used as historic controls. All of these patients presented with local or regional disease (stage I, II, or III) and later developed distant metastatic disease, for which they then received treatment. The time between metastases was treated as a time-to-event endpoint, and from these controls, the median time to second metastasis was estimated along with a pointwise estimate of the 95% confidence interval for the median time. We only included a highly analogous patient population from our historical controls. Cases that would not be eligible for the trial were eliminated, including those with profound immune suppression, and those who only had a single subsequent skin metastasis (these are often independent primary lesions or represent a very benign subset of patients). Statistical tests were performed with the Graph-Pad prism software version 3.0, with the R-package for statistical analysis (http://www.r-project.org), or SAS version 9.2.

Results

HLA-I upregulation followed by adoptive transfer of MCPyV-specific T cells induces regression of Merkel cell carcinoma

Pre- and post-treatment tumor tissue immunohistochemistry was used to evaluate viral oncoprotein expression, HLA-I expression and CD8 lymphocyte infiltration (Fig. 2A). As anticipated, the primary tumor and pre-treatment metastasis A biopsies were positive for the MCPyV T-Ag oncoprotein, but had weak or no HLA-I expression. In contrast, HLA-I was strongly up-regulated on the biopsy of the post-treatment metastasis (metastasis B) taken 146 days after the first treatment cycle, and as expected, MCPyV T-Ag expression was persistently maintained. Scattered $CD8^+$ T-cell infiltrates were detected in the primary tumor, as well as in the pre- and post-treatment biopsies (Fig. 2A).

Tumor burden and clinical efficacy were monitored using MRI and PET/CT scans (Fig. 2B). Immediately prior to the first treatment, the patient's initial pancreatic metastasis had enlarged, and 2 adjacent pancreatic tumors were newly detected compared to the scan performed 146 days earlier. Restaging 30 days after the first treatment showed that the largest lesion, which had undergone injection with IFNβ-Ib, had decreased in size, but the other two lesions had remained stable or increased in size. The best overall response by RECIST was a partial response (PR) observed following the second treatment consisting of localized, single dose 8 Gy radiation prior to T cell infusion and low-dose s.c IL-2. After the third treatment, 2 of 3 lesions continued to regress and one lesion remained refractory to treatment.

To determine systemic effects of adoptively transferred T cells, the time for new metastasis to develop after treatment was assessed in comparison to 49 historical matched controls undergoing standard, typically cytotoxic chemotherapy (Fig. 2C). The patient demonstrated no additional systemic metastasis until 535 days after the appearance of the first metastasis, which greatly exceeds the estimated median time of 200 days (95% confidence interval: 154–260 days) for development of new distant metastatic disease in historic controls. The scan performed 535 days after initial metastasis revealed new brain lesions that the patient declined to work-up. These likely represented MCC metastases, however as the patient also had a history of remote renal cell carcinoma and no biopsy was performed, metastasis from an RCC origin could not be excluded. Overall these data suggest the treatment induced regression in 2 of 3 metastases and may have contributed to a delay in the development of new distant disease.

Enhanced ability to respond to antigen after transfer of virus-specific CD8$^+$ T cells

The frequency and persistence of MCPyV-specific CD8 T cells in peripheral blood was assessed by their ability to bind the MCPyV-specific tetramer (Fig. 3A, **solid circles**). The frequency of these cells peaked 4–7 days after infusions (up to 8.8% of total CD8$^+$ T-cells) and remained detectable at the last assessment (219 days after the first treatment) at frequencies of ~1% which corresponded to a >3-fold increase compared to pre-infusion levels (0.26%).

We next assessed whether the virus-specific T cells detected after treatment were functional as assessed by their ability to secrete IFNγ in response to cognate peptide. Prior to the treatment cycles, cells that secreted IFNγ after exposure to the MCPyV peptide could not be detected within PBMC, suggesting that the MCPyV-specific cells binding to tetramer in the pre-treatment PBMC were non-functional. However, the frequency of CD8 T cells that secreted IFNγ in response to MCPyV peptide increased after each infusion (5.1, 4.5, and 3% after treatment 1, 2 and 3 respectively) and remained detectable at frequencies of ≥1% of total CD8$^+$ T-cells up to 219 days after the first infusion (Fig. 3A, **open circles**). Furthermore, the frequency of MCPyV-reactive peptide-responsive CD8$^+$ T cells correlated closely with the frequency of MCPyV tetramer-positive cells, suggesting that most of the persisting virus-specific cells remained functional *in vivo*.

As an increased frequency of virus-specific T cells over time may reflect antigen-specific cell division, we investigated whether the persisting MCPyV-specific T cells expressed Ki-67, a marker of proliferation (34). Prior to infusion, endogenous (pre-existing) MCPyV-specific T cells did not express Ki-67, indicating minimal/absent proliferation. Cells from the infusion product were overwhelmingly positive for Ki-67 (92% at day 14 after the last stimulation cycle *in vitro*), consistent with recent activation. Most transferred cells maintained Ki-67 expression early after transfer (>80% on day 1 after infusion) and, as expected, Ki-67 expression decreased after each infusion but remained well above baseline levels (Fig. 3B, **solid diamonds**) at 219 days after the first infusion. Ki-67 expression on MCPyV-specific CD8 T cells was overall significantly higher ($p=<0.005$) than Ki-67 expression of the host tetramer-negative CD8 T-cells (Fig. 3B, **open diamonds**), suggesting that the infused cells continued to divide in the presence of persistent antigen.

To validate the functional status and determine the differentiation profile of pre- and post-treatment virus-specific CD8 T cells, we evaluated the phenotype of the persisting transferred cells. Consistent with the absence of function and proliferation, both PD-1 (a marker of activation/exhaustion) and TIM-3 (a marker of exhaustion) were expressed on MCPyV-specific cells (90% and 78% respectively) found in PBMC before the treatment cycles, suggesting endogenous CD8 responses were dysfunctional and exhausted (Fig 3C and 3D). As expected, and following *ex vivo* expansion, the infusion product also expressed PD-1 (34%) and TIM-3 (93%). However, once infused into the patient, the transferred cells maintained PD-1 expression but lost Tim-3 expression such that cells found after transfer had a non-exhausted phenotype (Fig. 3C), consistent with their maintained function. Furthermore, seven days after transfer, 53% of MCPyV-specific cells transiently expressed CD137 (4-1BB), a marker associated with very recent activation (Fig. 3E).

Based on the absence of expression of the co-stimulatory molecule CD28, the IL-7 receptor CD127 as well as the lymph-node homing molecules CD62L and CCR7 (data not shown), the endogenous MCPyV-specific T cells found before infusions exhibited a differentiated effector memory phenotype (Fig. 3F and 3G). Consistent with the use of IL-21 in the *ex vivo* cultures (24–26), a subset of the infusion product generated for this patient expressed CD28 (78%) and CD127 (19%). After infusion into the patient, the transferred cells maintained CD28 expression (Fig. 3F) and further up-regulated CD127 (Fig. 3G). CD62L and CCR7

were not detected (data not shown). These data suggest that the transferred cells persisted with an effector memory phenotype (13), but in a less differentiated state compared to the endogenous response, with a maintained capacity to signal through CD28 and CD127. Regulatory T-cells (Tregs) can be sensitive to exogenous IL-2, and could negatively impact the persistence and function of transferred cytotoxic lymphocytes. Therefore, we assessed Treg numbers after infusions based on the expression of surrogate markers CD4 and CD25 and the absence of CD127 (24). Treg frequencies increased after each infusion from baseline levels but returned to near baseline levels within 28d of the infusion (Suppl. Fig. 3). In TIL, unfortunately, we were severely limited by the quantity of tissue available for analysis from the patient's metastases and therefore Treg analysis could not be performed.

Overall, adoptive transfer of polyclonal, MCPyV-specific T cells was associated with several key characteristics suggestive of an enhanced ability to respond to antigen: 1) markedly increased frequency of MCPyV-specific cells that persisted *in vivo*, 2) increased fraction of virus-reactive T cells, 3) ability to proliferate (Ki-67), 4) expression of activation markers (CD137, PD-1), and 5) facilitated co-stimulation and survival (CD28 and CD127) (35,36).

Transferred cells preferentially localize to metastatic MCC tissue

To capture the number and characteristics of the individual transferred MCPyV-specific $CD8^+$ T-cell clones, we analyzed tetramer-sorted infusion products, TIL, and PBMC for individual TCRβ CDR3 using high-throughput TCR DNA sequencing (32). The infusion product (which was sorted a second time to yield >99% pure $CD8^+$ $tetramer^+$ cells for TCRβ CDR3 analysis) was polyclonal and consisted of 502 individual virus-specific clonotypes. Three clonotypes were predominant and represented 99% of MCPyV-specific TCR reads (all three clones shared V-β7-9 and differed by their J-β subunits as depicted in Fig. 4A and 4B). We then used this method to determine all TCRβ CDR3 present in unsorted TIL and PBMC obtained before and after infusions and investigated whether the transferred virus-specific clonotypes were present within these samples, as well as their frequency. Prior to treatment, these three J-β variant clones were present amongst primary tumor TIL (0.03% J-β1-5, 0.06% J-β1-1, 2.8% J-β2-3) (Fig. 4C, **left panel**), and PBMC (0.06% J-β1-5, 0.15% J-β1-1, 0.01% J-β2-3) (Fig. 4D **left panel**), suggesting that these pre-existing clonotypes had been expanded in the PBMC-derived infusion product. Analysis of the post-treatment metastasis 146 days after the first infusion demonstrated that clone Jβ1-1 now represented 4.7% of all sequences, and the clones Jβ1-5 and Jβ2-3 were absent (Fig. 4C, **right panel**).

We then investigated whether additional clonotypes that were present in the post-treatment metastasis were also present within the low-prevalence MCPyV-specific clonotypes (<1%) in the infusion product. This analysis identified an additional MCPyV-specific clonotype (highlighted in red), with 1 nucleic-acid difference compared to the Jβ1-1 clonotype highlighted in blue that was present at 0.6% of all TCR reads in the post-treatment metastatic biopsy and absent in the pre-treatment TIL. However, because the frequency in the infusion product was so low (2.6×10-4%), we cannot formally exclude that this clone constituted a contaminant.

Overall, MCPyV-specific CD8 T-cell clonotypes present in the infused product increased from 2.9% in the primary tumor to 5.3% in the post-infusion metastasis (Fig. 4C). Two clones accounted for the increase in MCPyV-specific cells present in the biopsy metastasis following the treatments compared to the primary lesion. No increase in frequency of these three clones was observed in the peripheral blood before and after treatments at comparable time points (Fig. 4D, **right panels**). Using this method, the specificity of the majority of the clonotypes isolated from PBMC and TIL could not be determined and may have included 1) T cells specific for other MCPyV epitopes, 2) T cells recognizing non-viral TAAs such as

survivin (37), HIP1 oncoprotein that interacts with c-KIT (38), CD56, or other UV-induced mutational signatures, or 3) bystander or resident T cells. In summary, as the infusion product contained clones that aggregated at a higher frequency in the metastatic lesion compared to the peripheral blood, this suggests there was preferential localization of infused virus-specific T cells to the metastatic tissue.

Discussion

The purpose of this study was to investigate the efficacy and safety of HLA-I upregulating agents in combination with polyomavirus-specific adoptive T cell therapy in the setting of metastatic Merkel cell carcinoma. Even though pre-existing MCPyV-specific $CD8^+$ T-cells were present at low frequencies in the host prior to infusions (10), these were unable to prevent the rapid progression of metastatic disease. We addressed two key factors that may have contributed to the inefficiency of the endogenous virus-specific T cell responses: To reverse the observed down-regulated HLA-I expression on tumor cells necessary for the display of the MCPyV viral peptides, and render the cells accessible to specific T cell lysis, either intralesional IFNβ–1b and tumor-targeted, single-dose ionizing radiation (8 Gy) was administered 1–2 days before each T cell infusion. To address the absence of function of the endogenous CD8 responses, polyclonal MCPyV-specific CD8 T-cells were generated *ex vivo* from PBMC, expanded, and re-infused. This resulted in the increased frequency of detectable and functional CD8 T cells for over three months *in vivo* and preferential localization of the infused cells in tumor tissue as evidenced by TCR clonotype analysis. The combination of HLA-I upregulation followed by the infusion of MCPyV-specific CD8 T cells was well-tolerated and safe and mediated tumor regression in 2 of 3 detectable metastases consistent with T cell-mediated lysis. The absence of new metastatic disease in this patient for a prolonged period of time compared to historic controls also suggests that the treatment may have delayed or prevented the progression of distant metastatic disease. While the patient declined definitive work-up, it appears he developed metastatic MCC disease in the brain, a site with limited lymphocyte accessibility (39).

Although a clear increase in antitumor reactivity was achieved with this treatment, immune escape was not entirely halted. While regressing lesions in the pancreas could not be biopsied, the escaping pancreatic lesion was amenable to a limited fine need aspirate. Our data indicate that HLA-I and MCPyV T-Ag expression were maintained on the escaping lesion, thus their respective downregulation was eliminated as having played a role in immune evasion in the pancreas. Other mechanisms may have contributed to immune escape in some lesions in the patient. Infiltration of tumor tissue by $CD8^+$ T-cells has been shown to have a positive effect on survival in numerous cancer settings. TIL density and distribution were shown to independently predict sentinel lymph node status and survival in patients with melanoma (40,41). In MCC a clear correlation between $CD8^+$ T cell infiltration and favorable clinical outcome is established, consistent with a role for the recognition of tumor cells by host T-cells (14). In this patient, $CD8^+$ T cell infiltration in the primary tumor and pre- and post- treatment metastatic lesions remained scarce suggesting that other factors may have prevented $CD8^+$ infiltration and effective tumor lysis. A recent report suggests that vascular E-selectin within MCC tumors is critical in mediating intratumoral $CD8^+$ T cell infiltration (42); however, the intratumoral vascular architecture could not be assessed in this case. Furthermore, PD-1 expression has been shown to be higher in the tumor-infiltrating $CD8^+$ T cells and is associated with disease progression (43–45). Although transferred cells were PD-1^+ and functional in the peripheral blood, the function of the $CD8^+$ T cells infiltrating the tumor could not be assessed. Ultimately, more effective results might also be achieved by combining adoptive transfer with immunomodulatory strategies such as blockade of the PD-1/PD-L1 axis or anti-CTLA-4 blockade (46–48).

Similar to other virus-driven cancers, MCC is an attractive target for immunotherapy because characterized, non-self, non-cross-reactive antigens are constitutively expressed and necessary for tumor survival (3). The results of this single-patient study suggest that immune-mediated antitumor activity can be established with a very limited side effect profile and offers a strategy to rapidly elucidate the requirements for MCC tumor control directly in humans by bypassing the necessity of murine models (49,50). A multi-patient clinical trial is currently underway (NCT01758458) to further test this combinatorial immunotherapy approach using additional viral CD8 T cell epitopes in a broader cohort of MCC patients.

Supplementary Material

Refer to Web version on PubMed Central for supplementary material.

Acknowledgments

We would like to thank Dr. James A. DeCaprio for providing the MCPyV Large T-Ag antibody Ab3.

References

1. Henness S, Vereecken P. Management of Merkel tumours: an evidence-based review. Curr Opin Oncol. 2008; 20:280–6. [PubMed: 18391627]
2. Feng H, Shuda M, Chang Y, Moore PS. Clonal integration of a polyomavirus in human Merkel cell carcinoma. Science. 2008; 319:1096–100. [PubMed: 18202256]
3. Houben R, Shuda M, Weinkam R, Schrama D, Feng H, Chang Y, et al. Merkel cell polyomavirus-infected Merkel cell carcinoma cells require expression of viral T antigens. J Virol. 2010; 84:7064–72. [PubMed: 20444890]
4. Shuda M, Arora R, Kwun HJ, Feng H, Sarid R, Fernández-Figueras M-T, et al. Human Merkel cell polyomavirus infection I. MCV T antigen expression in Merkel cell carcinoma, lymphoid tissues and lymphoid tumors. Int J Cancer. 2009; 125:1243–9. [PubMed: 19499546]
5. Rodig SJ, Cheng J, Wardzala J, DoRosario A, Scanlon JJ, Laga AC, et al. Improved detection suggests all Merkel cell carcinomas harbor Merkel polyomavirus. The Journal of clinical investigation. 2012; 122:4645–53. [PubMed: 23114601]
6. Hadrup S, Donia M, Thor Straten P. Effector CD4 and CD8 T Cells and Their Role in the Tumor Microenvironment. Cancer Microenviron. 2012; 6:123–33. [PubMed: 23242673]
7. Chapuis AG, Thompson JA, Margolin KA, Rodmyre R, Lai IP, Dowdy K, Farrar EA, et al. Transferred melanoma-specific CD8+ T cells persist, mediate tumor regression, and acquire central memory phenotype. Proc Natl Acad Sci U S A. 2012; 109:4592–7. [PubMed: 22393002]
8. Heslop HE, Slobod KS, Pule MA, Hale GA, Rousseau A, Smith CA, et al. Long-term outcome of EBV-specific T-cell infusions to prevent or treat EBV-related lymphoproliferative disease in transplant recipients. Blood. 2009; 115:925–35. [PubMed: 19880495]
9. Hunder NN, Wallen H, Cao J, Hendricks DW, Reilly JZ, Rodmyre R, et al. Treatment of metastatic melanoma with autologous CD4+ T cells against NY-ESO-1. N Engl J Med. 2008; 358:2698–703. [PubMed: 18565862]
10. Iyer JG, Afanasiev OK, McClurkan C, Paulson K, Nagase K, Jing L, et al. Merkel cell polyomavirus-specific CD8(+) and CD4(+) T-cell responses identified in Merkel cell carcinomas and blood. Clin Cancer Res. 2011; 17:6671–80. [PubMed: 21908576]
11. Afanasiev OK, Yelistratova L, Miller N, Nagase K, Paulson K, Iyer JG, et al. Merkel Polyomavirus-Specific T Cells Fluctuate with Merkel Cell Carcinoma Burden and Express Therapeutically Targetable PD-1 and Tim-3 Exhaustion Markers. Clin Cancer Res. 2013; 19:5351–60. [PubMed: 23922299]
12. Wherry EJ, Teichgraber V, Becker TC, Masopust D, Kaech SM, Antia R, et al. Lineage relationship and protective immunity of memory CD8 T cell subsets. Nat Immunol. 2003; 4:225–34. [PubMed: 12563257]

13. Berger C, Jensen MC, Lansdorp PM, Gough M, Elliott C, Riddell SR. Adoptive transfer of effector CD8+ T cells derived from central memory cells establishes persistent T cell memory in primates. J Clin Invest. 2008; 118:294–305. [PubMed: 18060041]
14. Paulson KG, Iyer JG, Tegeder AR, Thibodeau R, Schelter J, Koba S, et al. Transcriptome-wide studies of merkel cell carcinoma and validation of intratumoral CD8+ lymphocyte invasion as an independent predictor of survival. J Clin Oncol. 2011; 29:1539–46. [PubMed: 21422430]
15. Haque M, Ueda K, Nakano K, Hirata Y, Parravicini C, Corbellino M, Yamanishi K. Major histocompatibility complex class I molecules are down-regulated at the cell surface by the K5 protein encoded by Kaposi's sarcoma-associated herpesvirus/human herpesvirus-8. J Gen Virol. 2001; 82:1175–80. [PubMed: 11297692]
16. Koopman LA, van Der Slik AR, Giphart MJ, Fleuren GJ. Human leukocyte antigen class I gene mutations in cervical cancer. J Natl Cancer Inst. 1999; 91:1669–77. [PubMed: 10511595]
17. Reits EA, Hodge JW, Herberts CA, Groothuis TA, Chakraborty M, Wansley EK, et al. Radiation modulates the peptide repertoire, enhances MHC class I expression, and induces successful antitumor immunotherapy. J Exp Med. 2006; 203:1259–71. [PubMed: 16636135]
18. Lee Y, Auh SL, Wang Y, Burnette B, Wang Y, Meng Y, et al. Therapeutic effects of ablative radiation on local tumor require CD8+ T cells: changing strategies for cancer treatment. Blood. 2009; 114:589–95. [PubMed: 19349616]
19. Boss JM. Regulation of transcription of MHC class II genes. Curr Opin Immunol. 1997; 9:107–13. [PubMed: 9039770]
20. Nakajima H, Takaishi M, Yamamoto M, Kamijima R, Kodama H, Tarutani M, Sano S. Screening of the specific polyoma virus as diagnostic and prognostic tools for Merkel cell carcinoma. J Dermatol Sci. 2009; 56:211–3. [PubMed: 19709861]
21. Yee C, Thompson JA, Byrd D, Riddell SR, Roche P, Celis E, Greenberg PD. Adoptive T cell therapy using antigen-specific CD8+ T cell clones for the treatment of patients with metastatic melanoma: In vivo persistence, migration, and antitumor effect of transferred T cells. Proc Natl Acad Sci U S A. 2002; 99:16168–73. [PubMed: 12427970]
22. National Cancer Institute NIoH. Cancer Therapy Evaluation Program. 2009. Common Terminology Criteria for Adverse Events (CTCAE) v4.0. 10/01/2009 ed
23. Ettinghausen SE, Moore JG, White DE, Platanias L, Young NS, Rosenberg SA. Hematologic effects of immunotherapy with lymphokine-activated killer cells and recombinant interleukin-2 in cancer patients. Blood. 1987; 69:1654–60. [PubMed: 3495302]
24. Chapuis AG, Ragnarsson GB, Nguyen HN, Chaney CN, Pufnock JS, Schmitt TM, et al. Transferred WT1-Reactive CD8+ T Cells Can Mediate Antileukemic Activity and Persist in Post-Transplant Patients. Science translational medicine. 2013; 5:174ra27.
25. Li Y, Bleakley M, Yee C. IL-21 influences the frequency, phenotype, and affinity of the antigen-specific CD8 T cell response. J Immunol. 2005; 175:2261–9. [PubMed: 16081794]
26. Li Y, Yee C. IL-21 mediated Foxp3 suppression leads to enhanced generation of antigen-specific CD8+ cytotoxic T lymphocytes. Blood. 2008; 111:229–35. [PubMed: 17921346]
27. Ho WY, Nguyen HN, Wolfl M, Kuball J, Greenberg PD. In vitro methods for generating CD8+ T-cell clones for immunotherapy from the naive repertoire. J Immunol Methods. 2006; 310:40–52. [PubMed: 16469329]
28. Riddell SR, Watanabe KS, Goodrich JM, Li CR, Agha ME, Greenberg PD. Restoration of viral immunity in immunodeficient humans by the adoptive transfer of T cell clones. Science. 1992; 257:238–41. [PubMed: 1352912]
29. Papagno L, Almeida JR, Nemes E, Autran B, Appay V. Cell permeabilization for the assessment of T lymphocyte polyfunctional capacity. J Immunol Methods. 2007; 328:182–8. [PubMed: 17920073]
30. Wang C, Sanders CM, Yang Q, Schroeder HW Jr, Wang E, Babrzadeh F, et al. High throughput sequencing reveals a complex pattern of dynamic interrelationships among human T cell subsets. Proc Natl Acad Sci U S A. 2010; 107:1518–23. [PubMed: 20080641]
31. Robins H, Desmarais C, Matthis J, Livingston R, Andriesen J, Reijonen H, et al. Ultra-sensitive detection of rare T cell clones. J Immunol Methods. 2012; 375:14–9. [PubMed: 21945395]

32. Robins HS, Campregher PV, Srivastava SK, Wacher A, Turtle CJ, Kahsai O, et al. Comprehensive assessment of T-cell receptor beta-chain diversity in alphabeta T cells. Blood. 2009; 114:4099–107. [PubMed: 19706884]
33. Allred DC, Harvey JM, Berardo M, Clark GM. Prognostic and predictive factors in breast cancer by immunohistochemical analysis. Mod Pathol. 1998; 11:155–68. [PubMed: 9504686]
34. Scholzen T, Gerdes J. The Ki-67 protein: from the known and the unknown. J Cell Physiol. 2000; 182:311–22. [PubMed: 10653597]
35. Boise LH, Minn AJ, Noel PJ, June CH, Accavitti MA, Lindsten T, Thompson CB. CD28 costimulation can promote T cell survival by enhancing the expression of Bcl-XL. Immunity. 1995; 3:87–98. [PubMed: 7621080]
36. Kimura MY, Pobezinsky LA, Guinter TI, Thomas J, Adams A, Park JH, et al. IL-7 signaling must be intermittent, not continuous, during CD8(+) T cell homeostasis to promote cell survival instead of cell death. Nature immunology. 2013; 14:143–51. [PubMed: 23242416]
37. Kim J, Mcniff JM. Nuclear expression of survivin portends a poor prognosis in Merkel cell carcinoma. Mod Pathol. 2008; 21:764–9. [PubMed: 18425079]
38. Ames HM, Bichakjian CK, Liu GY, Oravecz-Wilson KI, Fullen DR, Verhaegen M, et al. Huntingtin-Interacting Protein 1: A Merkel Cell Carcinoma Marker that Interacts with c-Kit. J Invest Dermatol. 2011:1–8. [PubMed: 21157415]
39. Engelhardt B, Ransohoff RM. The ins and outs of T-lymphocyte trafficking to the CNS: anatomical sites and molecular mechanisms. Trends Immunol. 2005; 26:485–95. [PubMed: 16039904]
40. Azimi F, Scolyer RA, Rumcheva P, Moncrieff M, Murali R, McCarthy SW, et al. Tumor-infiltrating lymphocyte grade is an independent predictor of sentinel lymph node status and survival in patients with cutaneous melanoma. J Clin Oncol. 2012; 30:2678–83. [PubMed: 22711850]
41. Gooden MJ, de Bock GH, Leffers N, Daemen T, Nijman HW. The prognostic influence of tumour-infiltrating lymphocytes in cancer: a systematic review with meta-analysis. Br J Cancer. 2011; 105:93–103. [PubMed: 21629244]
42. Afanasiev OK, Nagase K, Simonson W, Vandeven N, Blom A, Koelle DM, et al. Vascular E-Selectin Expression Correlates with CD8 Lymphocyte Infiltration and Improved Outcome in Merkel Cell Carcinoma. J Invest Dermatol. 2013; 133:2065–73. [PubMed: 23353989]
43. Ghebeh H, Barhoush E, Tulbah A, Elkum N, Al-Tweigeri T, Dermime S. FOXP3+ Tregs and B7-H1+/PD-1+ T lymphocytes co-infiltrate the tumor tissues of high-risk breast cancer patients: Implication for immunotherapy. BMC Cancer. 2008; 8:57. [PubMed: 18294387]
44. Poschke I, De Boniface J, Mao Y, Kiessling R. Tumor-induced changes in the phenotype of blood-derived and tumor-associated T cells of early stage breast cancer patients. International journal of cancer Journal international du cancer. 2012; 131:1611–20. [PubMed: 22190148]
45. Sfanos KS, Bruno TC, Meeker AK, De Marzo AM, Isaacs WB, Drake CG. Human prostate-infiltrating CD8+ T lymphocytes are oligoclonal and PD-1+ Prostate. 2009; 69:1694–703. [PubMed: 19670224]
46. Brahmer JR, Tykodi SS, Chow LQ, Hwu WJ, Topalian SL, Hwu P, et al. Safety and activity of anti-PD-L1 antibody in patients with advanced cancer. The New England journal of medicine. 2012; 366:2455–65. [PubMed: 22658128]
47. Topalian SL, Hodi FS, Brahmer JR, Gettinger SN, Smith DC, McDermott DF, et al. Safety, activity, and immune correlates of anti-PD-1 antibody in cancer. The New England journal of medicine. 2012; 366:2443–54. [PubMed: 22658127]
48. Hodi FS, O'Day SJ, McDermott DF, Weber RW, Sosman JA, Haanen JB, et al. Improved survival with ipilimumab in patients with metastatic melanoma. N Engl J Med. 2010; 363:711–23. [PubMed: 20525992]
49. Gomez BP, Wang C, Viscidi RP, Peng S, He L, Wu TC, Hung CF. Strategy for eliciting antigen-specific CD8+ T cell-mediated immune response against a cryptic CTL epitope of merkel cell polyomavirus large T antigen. Cell Biosci. 2012; 2:36. [PubMed: 23095249]
50. Zeng Q, Gomez BP, Viscidi RP, Peng S, He L, Ma B, et al. Development of a DNA vaccine targeting Merkel cell polyomavirus. Vaccine. 2012; 30:1322–9. [PubMed: 22210138]

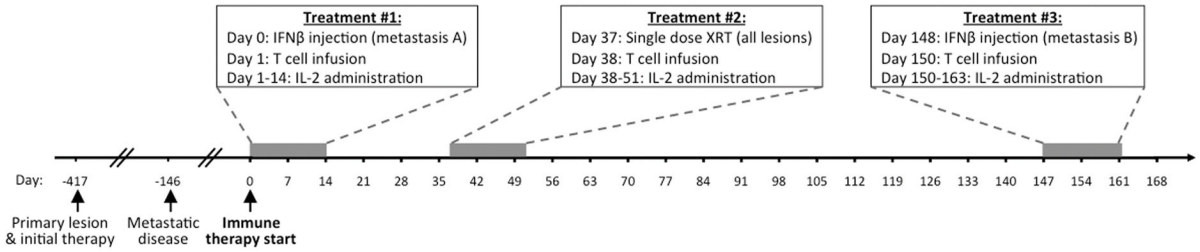

Figure 1. Timeline for disease presentation and immune therapy

Events as indicated relative to immune therapy start date. The patient received a total of three treatments that consisted of HLA-I upregulation (either intralesional injection of 3×10^6 IU of IFNβ-Ib or 8 Gy radiotherapy) followed by administration of $10^{10}/m^2$ MCPyV-specific polyclonal $CD8^+$ T cells and 14 days of twice daily subcutaneous injections of IL-2 (2.5×10^5 IU/m^2). XRT: radiotherapy.

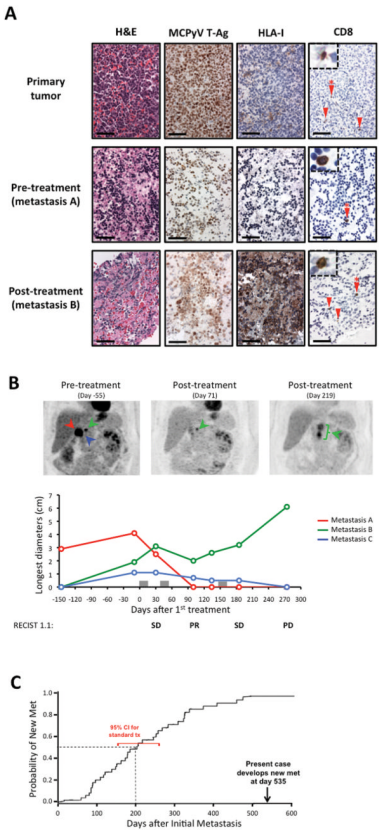

Figure 2. Response of individual MCC metastases after combined immune therapy

(A) Columns from left to right: Hematoxylin and Eosin stains, Immunohistochemistry for MCPyV T-Ag, HLA-I and CD8 (red arrows, red asterisk indicates cell in inset) of the primary tumor, pre-treatment (metastasis A, biopsied immediately prior to start of immune therapy) and post-treatment (metastasis B, biopsied 148 days after start of immune therapy) tumors. Scale bar = 50 μm. (B) MRI imaging (except the first datapoint, day −146, which was obtained by PET/CT) of individual metastases that included a peri-pancreatic lesion adjacent to the anterior duodenum (metastasis A, red), a pancreatic neck lesion (metastasis B, green) and a pancreatic head lesion (metastasis C, blue). The longest diameter in cm (y axis) of each metastasis is graphed over time (x axis). Representative images of pre- and post-treatment PET/CT scans are shown above the graph. Gray bars on x-axis indicate the timing of each treatment as detailed in Figure 1. The corresponding RECIST 1.1 criteria are indicated below the graph. (C) Kaplan-Meier curve of the probability of developing a second distant metastasis after the first detected metastasis (plotted at day zero) in 49 patients with MCC who developed distant disease. The 95% confidence interval is indicated in red.

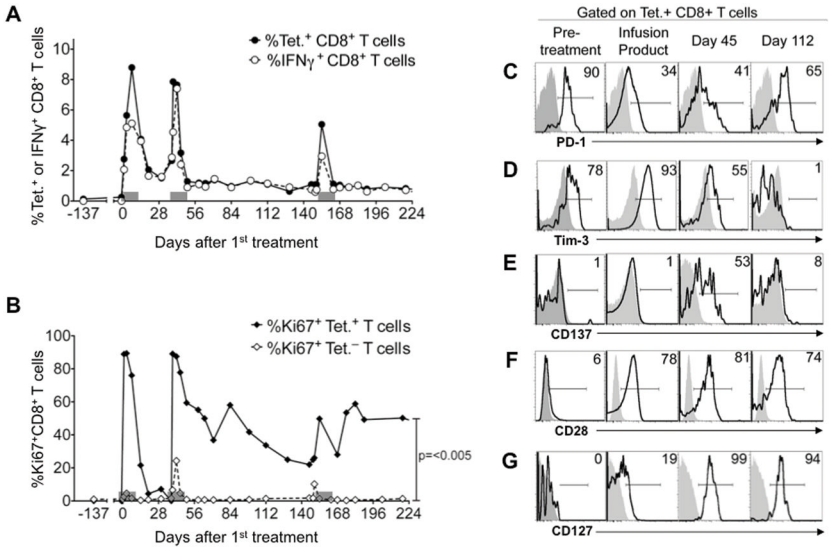

Figure 3. Persistence, function and phenotype of transferred MCPyV-specific CD8$^+$ T-cells

(A) Assessment of tetramer$^+$CD8$^+$ T-cells (%, solid circles, solid line) and IFNγ–reactive CD8$^+$ T-cells (%, open circles, dashed line) in PBMC collected at baseline (137 days and immediately prior to the first treatment) and at indicated timepoints after treatments. Gray bars on x-axis indicate the timing of each treatment as detailed in Figure 1. (B) Intranuclear Ki-67 expression on baseline and post-treatment CD8$^+$tetramer$^+$ cells (solid diamonds, solid line), and CD8$^+$tetramer$^-$ cells (open diamonds, dashed line). Gray bars on the x-axis indicated the timing of treatments as in (A) above. (C–G) Expression of PD-1, TIM-3, CD137, CD28 and CD127 on the infusion product, tetramer$^+$CD8$^+$ PBMC collected at baseline and after treatment as indicated. All parameters were acquired from multiple timepoints on the same day using the same negative control for each parameter as described in Methods, except for CD137 on day 45. A two-tailed paired t-test was used for statistical analysis.

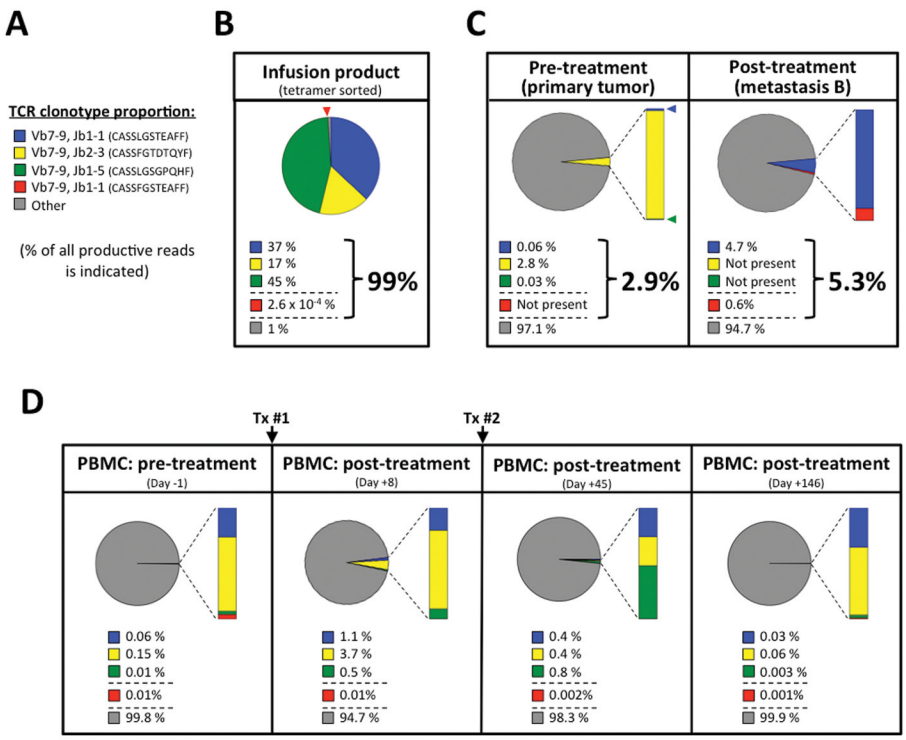

Figure 4. TCR clonotypic analysis for infused T cells and TIL within MCC tumors

(A) Legend for the four Vβ7-9 TCR clonotypes that were MCPyV-specific as assessed by HLA-A24-restricted MCPyV-specific tetramer binding. (B) Pie-chart indicating the individual TCRβ CDR3 clonotypes composing the $CD8^{+}$tetramer^{+} MCPyV-specific T cells isolated from the infusion product. Gray indicates other clonotypes found in the tetramer-sorted infusion product. (C) Pie-charts indicating the prevalence of the individual TCRβ CDR3 clonotypes present in the infusion product among all TCRβ CDR3 clonotypes isolated from expanded tumor-infiltrating lymphocytes from the primary tumor before treatment (left panel) and directly *ex vivo* from metastasis B after treatment (Day +148, right panel). The relative percentages of the individual clones are indicated. Gray indicates all other clonotypes found in the biopsy sample. (D) Pie-charts tracking the prevalence of the individual TCRβ CDR3 clonotypes among PBMC before and at several timepoints after treatment.